

Negative tunnel magnetoresistance in a quantum dot induced by interplay of a Majorana fermion and thermal-driven ferromagnetic leads

Peng-Bin Niu(牛鹏斌), Bo-Xiang Cui(崔博翔), and Hong-Gang Luo(罗洪刚)
Citation: Chin. Phys. B, 2021, 30 (**9**): 097401. DOI: 10.1088/1674-1056/abf10b
Journal homepage: http://cpb.iphy.ac.cn; http://iopscience.iop.org/cpb

What follows is a list of articles you may be interested in

Revealing the A_{1g}-type strain effect on superconductivity and nematicity in FeSe thin flake

Zhaohui Cheng(程朝晖), Bin Lei(雷彬), Xigang Luo(罗习刚), Jianjun Ying(应剑俊), Zhenyu Wang(王震宇), Tao Wu(吴涛), and Xianhui Chen(陈仙辉)
Chin. Phys. B, 2021, 30 (**9**): 097403. DOI: 10.1088/1674-1056/ac1efa

Superconductivity in an intermetallic oxide $Hf_3Pt_4Ge_2O$

Chengchao Xu(徐程超), Hong Wang(王鸿), Huanfang Tian(田焕芳), Youguo Shi(石友国), Zi-An Li(李子安), Ruijuan Xiao(肖睿娟), Honglong Shi(施洪龙), Huaixin Yang(杨槐馨), and Jianqi Li(李建奇)
Chin. Phys. B, 2021, 30 (**7**): 077403. DOI: 10.1088/1674-1056/abfb53

Doping effects of transition metals on the superconductivity of (Li,Fe)OHFeSe films

Dong Li(李栋), Peipei Shen(沈沛沛), Sheng Ma(马晟), Zhongxu Wei(魏忠旭), Jie Yuan(袁洁), Kui Jin(金魁), Li Yu(俞理), Fang Zhou(周放), Xiaoli Dong(董晓莉), and Zhongxian Zhao(赵忠贤)
Chin. Phys. B, 2021, 30 (**1**): 017402. DOI: 10.1088/1674-1056/abd2ab

Evidence for topological superconductivity: Topological edge states in Bi_2Te_3/FeTe heterostructure

Bin Guo(郭斌), Kai-Ge Shi(师凯歌), Hai-Lang Qin(秦海浪), Liang Zhou(周良), Wei-Qiang Chen(陈伟强), Fei Ye(叶飞), Jia-Wei Mei(梅佳伟), Hong-Tao He(何洪涛), Tian-Luo Pan(潘天洛), Gan Wang(王干)
Chin. Phys. B, 2020, 29 (**9**): 097403. DOI: 10.1088/1674-1056/abaf9c

Chiral p-wave pairing of ultracold fermionic atoms due to a quadratic band touching

Hai-Xiao Wang(王海啸), Zi-Heng Liu(刘子衡), Jian-Hua Jiang(蒋建华)
Chin. Phys. B, 2018, 27 (**2**): 027402. DOI: 10.1088/1674-1056/27/2/027402

Negative tunnel magnetoresistance in a quantum dot induced by interplay of a Majorana fermion and thermal-driven ferromagnetic leads*

Peng-Bin Niu(牛鹏斌)[1,†], Bo-Xiang Cui(崔博翔)[1], and Hong-Gang Luo(罗洪刚)[2,3]

[1] *Department of Physics, Shanxi Datong University, Datong* 037009, *China*
[2] *School of Physical Science and Technology, Lanzhou University, Lanzhou* 730000, *China*
[3] *Beijing Computational Science Research Center, Beijing* 100084, *China*

(Received 18 January 2021; revised manuscript received 23 February 2021; accepted manuscript online 23 March 2021)

We investigate the spin-related currents and tunnel magnetoresistance through a quantum dot, which is side-coupled with a Majorana fermion zero mode and two thermal-driven ferromagnetic electrodes. It is found that the interplay of Majorana fermion and electrodes' spin polarization can induce a nonlinear thermal-bias spin current. This interplay also decreases the total magnitude of spin or charge current, in either parallel or antiparallel configuration. In addition, a thermal-driven negative tunnel magnetoresistance is found, which is an unique feature to characterize Majorana fermion. With large temperature difference, a step phenomenon is observed in gate tuned spin-up current. When the coupling between quantum dot and topological superconductor is strong enough, this step will evolve into a linear relation, revealing Majorana fermion's robustness.

Keywords: Majorana fermion, spin current, tunnel magnetoresistance, thermal-bias

PACS: 74.25.F–, 74.25.fc, 85.75.–d, 72.25.–b **DOI:** 10.1088/1674-1056/abf10b

1. Introduction

The central theme of spintronics is to manipulate spin degrees of freedom in solid-state systems, to understand the interaction between the particle spin and its solid-state environments and to make useful devices.[1,2] In spintronics, generation of spin-polarized currents usually uses ferromagnetic electrodes[3–6] or central system's spin polarization.[7,8] The ferromagnetic electrodes have parallel or antiparallel configurations. With these configurations, the physical quantities can be measured by spin current, charge current or tunnel magnetoresistance (TMR).[9–11] Usually, the value of TMR is positive due to the charge current in parallel configuration is larger than the current in antiparallel configuration.[10] However, as will be seen below, the TMR can be negative when Majorana fermion is introduced.

Majorana fermions, with antiparticles being themselves, have been searched in high-energy physics for a long time.[12–14] The Majorana pair possesses topological properties, and in condensed matter physics it has been shown that the topology can be realized in many materials, such as topological insulators,[15,16] Bose–Einstein condensates,[17–19] Kagome lattice,[20,21] and silicene.[22] Recently, searches for Majorana fermions in condensed matter physics have attracted much attention, theoretically or experimentally,[23–30] due to the fact that they have non-Abelian statistics[31,32] and are promising in quantum computation. The predicted Majorana bound states, or Majorana zero modes correspond to the Majorana fermions in high-energy physics. They are coherent superpositions of hole and electron excitations of zero energy, which can be realized at the two ends of a topological superconductor wire.[33,34] In quantum transport, the readout and manipulation of Majorana zero mode in quantum dot-Majorana hybrid systems[35–39] have been extensively studied and many interesting results are found. For example, the presence of Majorana zero mode leads to a quantized 1/2 zero-bias conductance[35] $G = 2e^2/h$, when the dot is on resonance and symmetrically coupled to the probing leads.

Motivated by these achievements, in this paper we consider temperature-driven spin-polarized quantum transport in a quantum dot-Majorana hybrid system connected with ferromagnetic electrodes. The polarization are generated from two factors: the central system's spin polarization induced by Majorana zero mode and the ferromagnetic electrodes' spin polarization. It is shown that the interplay of Majorana fermion and electrodes' spin polarization leads to some interesting results. For instance, we find that the interplay can induce nonlinear thermal-driven spin current. A thermal-driven negative tunnel magnetoresistance is also found. With large temperature difference and strong coupling between quantum dot and topological superconductor, the relationship between spin-up current and gate voltage becomes linear, revealing Majorana fermion's robustness.

This paper is organized as follows. In Section 2 we describe the model of quantum dot coupled with Majorana

*Project supported by the National Natural Science Foundation of China (Grant Nos. 11834005 and 11674139).
†Corresponding author. E-mail: niupengbin@163.com
© 2021 Chinese Physical Society and IOP Publishing Ltd

fermion zero mode. Specific Hamiltonian, basic formula for currents and TMR are presented there. In Section 3 we present the numerical results and explain the behaviors of spin-related currents and TMR. Finally, Section 4 is devoted to a brief conclusion.

2. Model and method

We consider a system shown in Fig. 1. It consists of a spin-degenerate quantum dot (QD) side-coupled with a topological superconductor wire, which supports two Majorana fermion zero modes. It is assumed that the length of the topological superconductor wire is larger than the superconducting coherence length, so that the overlap and interaction between the pair of two Majorana zero modes are neglected.[40] The QD is also coupled to two thermal-driven ferromagnetic leads. The Hamiltonian can be written as[35–40]

$$H = \sum_{k\sigma\alpha} \varepsilon_{k\alpha} c^{\dagger}_{k\alpha\sigma} c_{k\alpha\sigma} + \sum_{k\alpha\sigma} (t_{k\alpha\sigma} c^{\dagger}_{k\alpha\sigma} d_{\sigma} + \text{H.c.}) + \sum_{\sigma} \varepsilon_0 d^{\dagger}_{\sigma} d_{\sigma} + \lambda (d_{\uparrow} - d^{\dagger}_{\uparrow}) \gamma_1, \quad (1)$$

where the first term in Eq. (1) describes the left and right leads; $c^{\dagger}_{k\alpha\sigma}(c_{k\alpha\sigma})$ is the electronic creation (annihilation) operator with momentum k, spin σ, and energy $\varepsilon_{k\alpha}$ in the electrodes $\alpha = \mathrm{L},\mathrm{R}$. The second term describes the coupling between the dot and the ferromagnetic leads; $t_{k\alpha\sigma}$ describes the spin-dependent tunneling amplitude between quantum dot and leads. The third terms in Eq. (1) describe the spinful quantum dot. The operators d_{σ} and $d^{\dagger}_{\sigma}$ denote annihilation and creation of a quantum dot electron with spin σ and gate tunable energy level ε_0. The last term in Eq. (1) describes the coupling between the dot and the Majorana zero mode (MZM), where λ is the coupling parameter and γ_1 describe the MZM, which have developed at the edges of the topological nanowire. Because of MZM's helical property, only one of the dot spin degrees of freedom (chosen as spin-up) is coupled to the MZM.[39]

The standard equation of motion method yields the exact expression for the spin-up Green's function[35]

$$\langle\langle d_{\uparrow} | d^{\dagger}_{\uparrow} \rangle\rangle = \frac{1}{\omega - \varepsilon_0 - \Sigma^{\uparrow}_0 - 2\lambda^2 K(\omega)[1 + 2\lambda^2 \tilde{K}(\omega)]}, \quad (2)$$

where $K(\omega) = 1/\omega$ and $\tilde{K}(\omega) = K(\omega)/[\omega + \varepsilon_0 - \Sigma^{\uparrow}_0 - 2\lambda^2 K(\omega)]$. $\Sigma^{\uparrow}_0 = \sum_{k\alpha} |t_{k\alpha\uparrow}|^2/(\omega - \varepsilon_{k\alpha} + \mathrm{i}\eta)$ is the spin-up self-energy induced by the coupling between ferromagnetic leads and QD. Under the wide band approximation, the self-energy is calculated by[10] $\Sigma^{\uparrow}_0 = -\mathrm{i}(\Gamma^{\uparrow}_{\mathrm{L}} + \Gamma^{\uparrow}_{\mathrm{R}})/2$, with $\Gamma^{\sigma}_{\mathrm{L/R}} = \Gamma(1 + \sigma p)$ for ferromagnetic leads' parallel configuration. For antiparallel configuration, $\Gamma^{\sigma}_{\mathrm{L}} = \Gamma(1 + \sigma p)$ and $\Gamma^{\sigma}_{\mathrm{R}} = \Gamma(1 - \sigma p)$. Γ is the line-width constant, and p is the spin-polarization parameter.

For spin-down Green's function, it is easy to obtain

$$\langle\langle d_{\downarrow} | d^{\dagger}_{\downarrow} \rangle\rangle = \frac{1}{\omega - \varepsilon_0 - \Sigma^{\downarrow}_0}. \quad (3)$$

Within the non-equilibrium Green's function formalism, the transport current is expressed as[41,42]

$$I_{\sigma} = \frac{e}{\hbar} \int \mathrm{d}\omega \frac{\Gamma^{\sigma}_{\mathrm{L}} \Gamma^{\sigma}_{\mathrm{R}}}{\Gamma^{\sigma}_{\mathrm{L}} + \Gamma^{\sigma}_{\mathrm{R}}} [f_{\mathrm{L}}(\omega) - f_{\mathrm{R}}(\omega)] \rho_{\sigma}(\omega), \quad (4)$$

where $\rho_{\sigma}(\omega) = -(1/\pi)\mathrm{Im}G^{\mathrm{r}}_{\sigma}(\omega)$ is the spectral function; $G^{\mathrm{r}}_{\sigma}(\omega) = \langle\langle d_{\sigma} | d^{\dagger}_{\sigma} \rangle\rangle$ is the on-site retarded Green's function; $f_{\alpha}(\omega) = \{\exp[(\omega_0)/k_{\mathrm{B}}T] + 1\}^{-1}$ is the Fermi–Dirac distribution function. Thermal-driven currents generate from temperature difference in left and right leads. We take $T_{\mathrm{L}} = \theta + T_{\mathrm{R}}$, where T_{R} is taken as background temperature and θ denotes the temperature difference. From Eq. (4), the corresponding spin current[43,44] and charge current are given as $I_{\mathrm{s}} = I_{\uparrow} - I_{\downarrow}$ and $I_{\mathrm{c}} = I_{\uparrow} + I_{\downarrow}$. In the following, we denote the charge current as I_{P} for ferromagnetic leads' parallel configuration, and I_{AP} for antiparallel configuration.

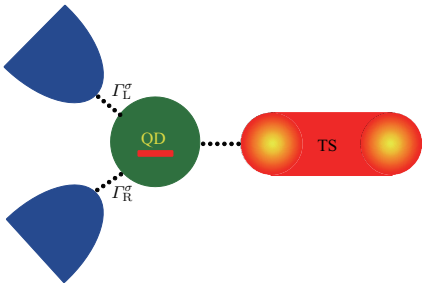


Fig. 1. Schematic depiction of the model under consideration. The system is placed between two ferromagnetic electrodes with spin-dependent coupling Γ^{σ}_{α}. It consists of a quantum dot and a topological superconductor which supports Majorana fermion zero modes. One of the quantum dot's spins is side-coupled with a Majorana zero mode (MZM) (see Hamiltonian in the text). The electrodes is applied with a temperature difference.

The spin-polarized transport properties, especially the tunnel magnetoresistance (TMR) effect, have been proven to be useful in information-storage devices. TMR is quantitatively characterized as[10]

$$\mathrm{TMR} = (I_{\mathrm{P}} - I_{\mathrm{AP}})/I_{\mathrm{AP}}. \quad (5)$$

3. Results and discussion

In the following we investigate the transport properties induced by the interplay of Majorana fermion and electrodes' spin polarization. Based on the formulas of currents and TMR, the numerical results are provided.

Firstly, in Fig. 2 we consider the spin current I_{s} and charge current I_{P} (I_{AP}) for parallel (antiparallel) configuration, as a function of the temperature difference θ. We start first to analyze the behaviors of spin current with electrodes' parallel configuration in Fig. 2(a). When $p = 0$ and $\lambda = 0$, i.e., when there are no spin polarization and Majorana fermion, the magnitudes of spin-up and spin-down currents are equal, hence the spin

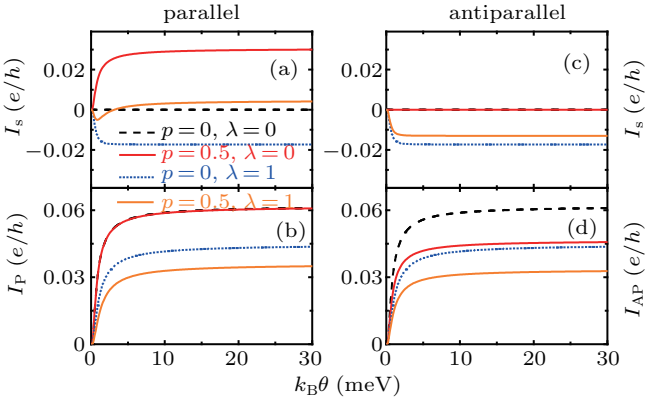


Fig. 2. Spin current and charge current as a function of temperature difference for parallel configuration [(a), (b)] and antiparallel configuration [(c), (d)]. The spin polarization and QD-MZM coupling strength in (a)–(d) are kept to be unchanged. In comparison, the curves for $p=0$ are also presented (dashed and dotted lines). The other parameters are $\varepsilon_0=1, \Gamma=0.02$. The background temperature is chosen as $k_BT=0.01$. All energies are in units of meV.

current is zero. When the QD–MZM coupling appears ($p=0$ and $\lambda=1$), one can observe a negative thermal-driven spin current. This is because the appearance of Majorana fermion decreases spin-up current and induces a negative spin current. However, when $p\neq 0$ and $\lambda=0$, one can observe a positive spin current, because the majority spin-up electrons can flow through the QD with parallel configuration. Thus the interplay of Majorana fermion and spin polarization induces a nonlinear spin current, which decreases first and then increases, as seen in Fig. 2(a) with $p=0.5$ and $\lambda=1$. Although ferromagnetic leads' spin polarization induces spin-up majority and spin-down minority, itself alone does not affect the total magnitude of the charge current. Thus in Fig. 2(b) the two curves ($p=0,\lambda=0$ and $p=0.5,\lambda=0$) overlap. As shown in Fig. 2(a), the QD–MZM coupling alone will decrease charge current, as seen in Fig. 2(b) for $p=0$, $\lambda=1$. However, the union (or interplay) of Majorana fermion and spin polarization will further decrease the charge current, as seen in Fig. 2(b) for $p=0.5$, $\lambda=1$. In the meantime, one can see from Fig. 2(d) that the charge current also has the minimal magnitude for $p=0.5$, $\lambda=1$. Therefore, we can conclude that the interplay decreases the total magnitude of the charge current, in either parallel or antiparallel configuration. We then analyze the behaviors of currents with antiparallel configuration. The antiparallel configuration alone does not induce spin current, instead it decreases the total magnitude of the charge current, as seen in Figs. 2(c) and 2(d). The QD–MZM coupling alone will decrease spin-up current, and generate negative spin current. However, the interplay of Majorana fermion and spin polarization will further decrease the spin current, as seen in Fig. 2(c).

From Fig. 2 one can see a characteristic of the thermal-driven currents: with large enough temperature difference, the currents tend towards stability, i.e., thermal bias will not affect the currents anymore, and in this situation the currents will be sensitive to gate voltage (or ε_0). Hence in Fig. 3 we discuss the currents with varying gate voltage for fixed large temperature difference. In Fig. 3 we focus on the behaviors of spin-up current $I_\uparrow$ (in which Majorana fermion appears and exhibit an interesting result, as will be shown below) and spin current I_s.

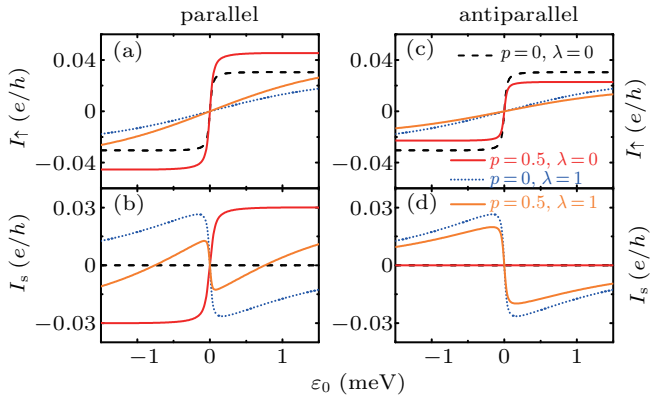


Fig. 3. Spin-up current $I_\uparrow$ and spin current I_s as a function of energy level ε_0 for parallel configuration [(a), (b)] and antiparallel configuration [(c), (d)]. The spin polarization and QD–MZM coupling strength in (a)–(d) are kept to be constant. In comparison, the curves for $p=0$ are also presented (dashed and dotted lines). The other parameters are $\theta=30$, $\Gamma=0.02$. The background temperature is chosen as $k_BT=0.01$. All energies are in units of meV.

Let us discuss the spin-resolved current first. In Figs. 3(a) and 3(c), for the curves of $\lambda=0$, one sees a step located at $\varepsilon_0=0$, where the gate tunable energy level ε_0 passes through the Fermi surface. When $\varepsilon_0<0$, there is a heat-generated current flowing from right lead to left (which is negative). When $\varepsilon_0>0$, there is a positive current flowing from left to right. It should be pointed out that in bias-driven quantum transport the phenomenon of step in current is also observed, where the gate voltage is fixed. Here the situation is opposite. An interesting result found here is that when $\lambda=1$, the step disappears and the functional relation between spin-up current and energy level becomes linear. This reveals Majorana fermion's robustness. Due to this linear relationship, i.e., Majorana fermion's robustness, the spin currents for $\lambda=1$ show an antisymmetric oscillating structure, as seen in Figs. 3(b) and 3(d). The union of Majorana fermion and spin polarization decreases the magnitude of current, which is verified again in Figs. 3(b) and 3(d). Interestingly, the spin current has three zero points for parallel configuration, while in the case of antiparallel configuration or zero spin polarization, the spin current has only one zero point.

In Fig. 4 we present the TMR as a as a function of temperature difference. In Fig. 4(a) we consider the thermal-driven TMR without MZM. At $\theta=0$, the TMR starts with the Julliere value[3,10] $2p^2/\left(1-p^2\right)$. Increasing the temperature of left lead, TMR reduces to $p^2/\left(1-p^2\right)$, meaning that the transport channel ε_0 is active. As a comparison, when $\lambda\neq 0$, i.e., the interplay of Majorana fermion and spin polarization is introduced, one observes a sign change of TMR, the position of which is related with the energy level ε_0. In the meantime, one can see a negative TMR. The sign change and negative TMR

are induced by the alternately change of $I_{\rm P}$ and $I_{\rm AP}$, which is originated from the interplay. This sign change and negative TMR are unique and can be counted as a fingerprint of Majorana fermion.

In Fig. 5 the TMR varying with energy level ε_0 is presented. In Fig. 5(a) the TMR without Majorana fermion is shown. The TMR changes intensely around $\varepsilon_0 = 0$, when it passes through the Fermi level. The whole curve of TMR is positive, because $I_{\rm P} > I_{\rm AP}$. In Fig. 5(b) the TMR with QD-MZM coupling and spin polarization is plotted. It is seen that the gated-tuned TMR with fixed large temperature difference exhibits a symmetric structure, and two regions of negative TMR are observed, which is accompanied with multiple sign changes.

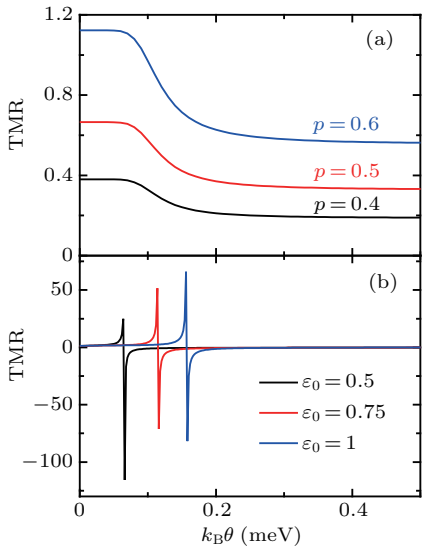


Fig. 4. Tunnel magnetoresistance (TMR) as a function of temperature difference. The parameters used in (a) are $\varepsilon_0 = 1$, $\lambda = 0$, $p = 0.4/0.5/0.6$, and in (b) are $\lambda = 0.5$, $p = 0.5$, $\varepsilon_0 = 0.5/0.75/1$. The other parameters are $\Gamma = 0.02$ and background temperature $k_{\rm B}T = 0.01$. All energies are in units of meV.

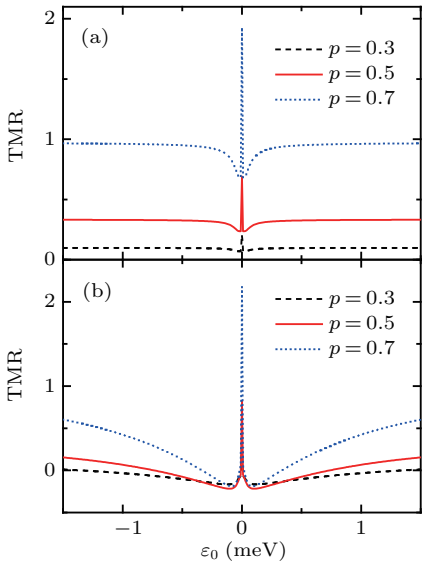


Fig. 5. Tunnel magnetoresistance (TMR) as a function of energy level ε_0 for (a) $\lambda = 0$ and (b) $\lambda = 1$. The spin polarizations in (a) and (b) are the same, as indicated. The other parameters are $\theta = 30$, $\Gamma = 0.02$, and background temperature $k_{\rm B}T = 0.01$. All energies are in units of meV.

4. Conclusions

In summary, we have used an exactly solvable model to discuss thermal-driven quantum transport involved with the interplay of Majorana fermion and spin polarization. It is found that the interplay of Majorana fermion and spin polarization can induce a nonlinear thermal-bias spin current. A thermal-driven negative tunnel magnetoresistance is also found. With large temperature difference, the gate tuned spin-up current becomes linear, when the coupling between quantum dot and topological superconductor is strong enough, revealing Majorana fermion's robustness. These results may be useful in the future design of thermal-based spintronic devices.

References

[1] Zutić I and Sarma S D 2004 *Rev. Mod. Phys.* **76** 323
[2] Hanson R, Kouwenhoven L P, *et al.* 2007 *Rev. Mod. Phys.* **79** 1217
[3] Julliere M 1975 *Phys. Lett. A* **54** 225
[4] Trocha P, Weymann I and Barnas J 2009 *Phys. Rev. B* **80** 165333
[5] Chi F, Dai X N and Sun L L 2010 *Appl. Phys. Lett.* **96** 082102
[6] Zhang S N, Zhu W H, *et al.* 2018 *Acta Phys. Sin.* **67** 197202 (in Chinese)
[7] Niu P B, Liu L X, *et al.* 2018 *AIP Adv.* **8** 015215
[8] Niu P B, Liu L X, *et al.* 2020 *J. Magn. Magn. Mater.* **506** 166795
[9] Rudzinski W and Barnas J 2001 *Phys. Rev. B* **64** 085318
[10] Weymann I, Konig J, *et al.* 2005 *Phys. Rev. B* **72** 115334
[11] Yu Y, Hu W J, *et al.* 2020 *Chin. Phys. B* **29** 018501
[12] Majorana E 1937 *Nuovo Cimento* **14** 171
[13] Nayak C, Simon S H, *et al.* 2008 *Rev. Mod. Phys.* **80** 1083
[14] Stern A 2010 *Nature* **464** 187
[15] Chang C Z, Zhang J S, *et al.* 2013 *Science* **340** 167
[16] He K, Wang Y and Xue Q K 2014 *Natl. Sci. Rev.* **1** 38
[17] Wang L, Liu J S, *et al.* 2020 *Acta Phys. Sin.* **69** 010303 (in Chinese)
[18] Li J and Liu W M 2018 *Acta Phys. Sin.* **67** 110302 (in Chinese)
[19] Liu J S, Li J and Liu W M 2017 *Acta Phys. Sin.* **66** 130305 (in Chinese)
[20] Chen Y H, Tao H S, Yao D X and Liu W M 2012 *Phys. Rev. Lett.* **108** 246402
[21] Jiang Z F, Li R D, Zhang S C and Liu W M 2005 *Phys. Rev. B* **72** 045201
[22] Zhang X L, Liu L F and Liu W M 2005 *Sci. Rep.* **3** 2908
[23] Reich E S 2012 *Nature* **483** 132
[24] Brouwer P W 2012 *Science* **336** 989
[25] Wilczek F 2012 *Nature* **486** 195
[26] Albrecht S M, Higginbotham A P, *et al.* 2016 *Nature* **531** 206
[27] Sun H H, Zhang K W, *et al.* 2016 *Phys. Rev. Lett.* **116** 257003
[28] He Q L, Pan L, *et al.* 2017 *Science* **357** 294
[29] Jeon S, Xie Y, Li J, Wang Z, Bernevig B A and Yazdani A 2017 *Science* **358** 772
[30] Chen H J 2020 *Quantum Inf. Process.* **19** 171
[31] Read N and Green D 2000 *Phys. Rev. B* **61** 10267
[32] Ivanov D A 2001 *Phys. Rev. Lett.* **86** 268
[33] Lutchyn R M, Sau J D and Sarma D S 2010 *Phys. Rev. Lett.* **105** 077001
[34] Oreg Y, Refael G and von Oppen F 2010 *Phys. Rev. Lett.* **105** 177002
[35] Liu D E and Baranger H U 2011 *Phys. Rev. B* **84** 201308
[36] Napitu B D 2015 *Eur. Phys. J. B* **88** 290
[37] Lü H F, Lu H Z and Shen S Q 2014 *Phys. Rev. B* **90** 195404
[38] Liu D E, Cheng M and Lutchyn R M 2015 *Phys. Rev. B* **91** 081405
[39] Huo D M 2016 *Eur. Phys. J. B* **89** 174
[40] Weymann I 2017 *J. Phys.: Condens. Matter* **29** 095301
[41] Jauho A P, Wingreen N S and Meir Y 1994 *Phys. Rev. B* **50** 5528
[42] Martinek J, Utsumi Y, *et al.* 2003 *Phys. Rev. Lett.* **91** 127203
[43] Wang R Q, Sheng L, Shen R, Wang B and Xing D Y 2010 *Phys. Rev. Lett.* **105** 057202
[44] Feng X Y, Zhang Q H, *et al.* 2019 *Chin. Phys. B* **28** 107105